Canadian Mineralogist
Vol. 28, pp. 629-638 (1990)

FLUID-INCLUSION EVIDENCE FOR THE PHYSICAL AND CHEMICAL CONDITIONS ASSOCIATED WITH INTERMEDIATE-TEMPERATURE PGE MINERALIZATION AT THE NEW RAMBLER DEPOSIT, SOUTHEASTERN WYOMING

MATTHEW W. NYMAN, RONALD W. SHEETS AND ROBERT J. BODNAR
Department of Geological Sciences, Virginia Polytechnic Institute and State University, Blacksburg, Virginia 24061 U.S.A.

ABSTRACT

The New Rambler Pt–Cu–Au deposit, Wyoming, is frequently cited as the type example of intermediate-temperature (200–700°C) remobilization of *PGE* by hydrothermal fluids. Fluid inclusions found in variably deformed quartz segregations associated with propylitic (chlorite + epidote + clinozoisite + albite + magnetite ± pyrite) and phyllic (quartz + sericite + pyrite) alteration assemblages record a minimum temperature of 335°C for the associated *PGE* mineralization. Types of fluid inclusions include, in chronological order of trapping, N_2, CO_2 ($\pm H_2O$) and H_2O–NaCl–$CaCl_2$. The latter inclusions have been separated into high-salinity and low-salinity subgroups. The close temporal and spatial association of high-salinity H_2O–NaCl–$CaCl_2$ fluid inclusions with propylitic and phyllic alteration assemblages supports *PGE* transport as chloride complexes. Theoretical calculations of Pt and Pd solubility also support the potential for chloride complexing. The observed fluid-inclusion compositions are similar in some respects to those observed in hydrothermal portions of the Bushveld, where *PGE* transport as chloride complexes at higher (>700°C) temperatures has been postulated.

Keywords: New Rambler deposit, hydrothermal *PGE* deposit, fluid inclusions, Wyoming.

SOMMAIRE

Le gisement à Pt–Cu–Au de New Rambler, au Wyoming, est souvent cité comme exemple type de remobilisation des éléments du groupe du platine (*EGP*) dans un milieu hydrothermal à température intermédiaire (entre 200 et 700°C). Les inclusions fluides, présentes dans des ségrégations de quartz plus ou moins déformé associées aux assemblages de zones d'altération propylitique (chlorite + épidote + clinozoïsite + albite + magnétite ± pyrite) et phyllique (quartz + séricite + pyrite), témoignent d'une température minimale de 335°C pour la minéralisation en *EGP*. Les types d'inclusions fluides comprennent, dans l'ordre chronologique de leur occlusion, N_2, CO_2 ($\pm H_2O$), et H_2O–NaCl–$CaCl_2$. Nous avons séparé les inclusions tardives en sous-groupes selon leur salinité. L'étroite association temporelle et spatiale des inclusions à forte salinité et à H_2O–NaCl–$CaCl_2$ avec les assemblages d'altérations propylitique et phyllique fait penser que le transfert des *EGP* s'est effectué sous forme de complexes chlorurés. Les calculs théoriques de la solubilité de Pt et Pd confirment également la capacité des complexes chlorurés. Les compositions observées des inclusions fluides ressemblent en certains points à celles des domaines hydrothermaux du complexe du Bushveld, où le transfert des éléments du groupe du platine sous forme de complexes chlorurés à température plus élevée (>700°C) a déjà été proposé.

(Traduit par la Rédaction)

Mots-clés: gisement de New Rambler, éléments du groupe du platine, gisement hydrothermal, inclusions fluides, Wyoming.

INTRODUCTION

Hydrothermal platinum-group elements (*PGE*) deposits have been recognized in a variety of environments that can be subdivided based on the temperature of mineralization. Examples of high-temperature (>700°C) deposits include pothole and stratiform *PGE* deposits in the Bushveld (Stumpfl 1986, Stumpfl & Ballhaus 1986, Schiffries 1982, Schiffries & Skinner 1987) and the Stillwater (Boudreau *et al.* 1986) layered mafic intrusions. Current models for the genesis of high-temperature deposits involve transport of *PGE* and associated metals by chloride complexes during late-stage magmatic–hydrothermal processes. Intermediate-temperature (200–700°C) *PGE* deposits occur within shear zones cutting mafic to ultramafic rocks and include the New Rambler deposit (McCallum *et al.* 1976, Loucks 1976) and the Rathbun Lake deposit (Rowell & Edgar 1986). Low-temperature (<200°C) deposits include the Kuperschiefer deposit in eastern Europe (Kucha 1982) and the Coronation Hill deposit, Northern Territory, Australia (Needham & Stuart-Smith 1987). Recent experimental (Orlova *et al.* 1987) and theoretical studies (Mountain & Wood 1988, Sassini & Shock 1990) indicate that *PGE* may be more mobile in aqueous solutions than previously recognized (Cousins 1973).

The New Rambler deposit formed as a result of *PGE* leaching from mafic wallrocks by hydrothermal fluids, and deposition of platinum-group minerals (*PGM*) and associated sulfides within the deformed mafic rocks (McCallum *et al.* 1976, Loucks 1976). Evidence cited for a hydrothermal origin includes: (1) ore textures indicative of replacement during hydrothermal processes, (2) association between *PGM* and hydrothermal alteration assem-

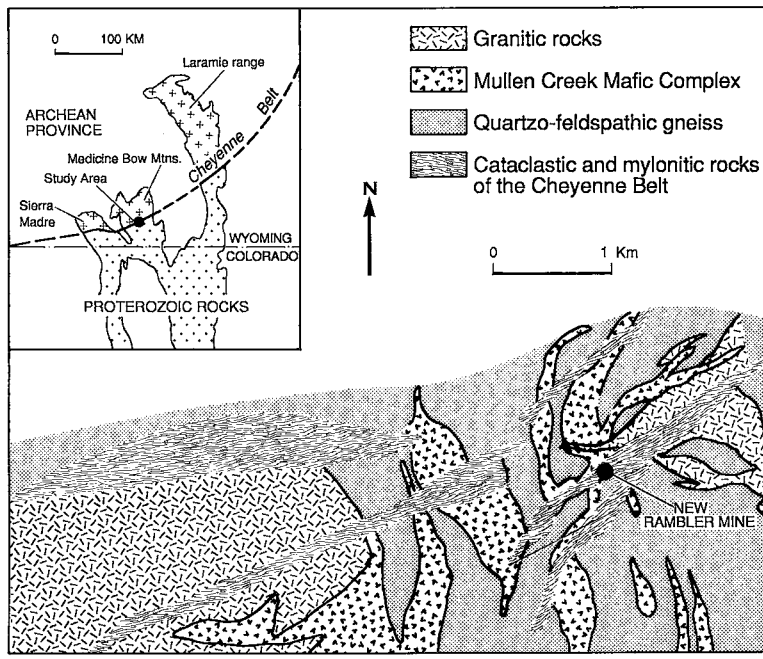

FIG. 1. Geological map of the area surrounding the New Rambler deposit, adapted from Houston (1968). Inset map shows regional geology of the Cheyenne belt and Precambrian rocks of southeastern Wyoming, after Duebendorfer & Houston (1987).

blages, (3) higher concentrations of soluble (Pd and Pt) relative to less soluble (Ru, Rh, Os, and Ir) *PGE*, and (4) enrichment of other elements (Bi, Cu, Au, and Ag) in the ore compared to the unaltered host-rock.

The New Rambler deposit is considered the type example for intermediate-temperature remobilization of *PGE* (Macdonald 1987, Mountain & Wood 1988); yet, little is known concerning the composition of mineralizing fluids and the *P–T* conditions of ore deposition. In this study, fluid inclusions trapped in quartz segregations within the hydrothermally altered wallrock were examined. Microthermometric data, physical and chemical constraints from ore and wallrock assemblages, and theoretical and experimental data are used to delineate the conditions of mineralization.

GEOLOGICAL FRAMEWORK

Regional geology

The New Rambler deposit is located in the Medicine Bow Mountains, in southeastern Wyoming (Fig. 1), within an east–west splay of the Cheyenne belt. The Cheyenne belt, formerly called the Mullen Creek – Nash Fork shear zone, is a northeast-trending tectonic boundary that can be traced from the Medicine Bow Mountains westward to the Sierra Madre Range and eastward to the Laramie Range. The Cheyenne belt also is a distinct geochronological boundary separating Archean basement, which is overlain by a Proterozoic miogeosynclinal sequence, to the northwest, from Proterozoic metavolcanic and plutonic, greenschist- to amphibolite-grade terranes to the southeast. Within the Medicine Bow Mountains, the Cheyenne belt is characterized by several distinct lithotectonic blocks that are separated by zones of ductile shear, with both cataclastic and crystal-plastic fabrics. Deformation along the Cheyenne belt involved northwestward thrusting during a Proterozoic accretionary event followed by lower-grade strike-slip movement (Duebendorfer & Houston 1987). Deformation during the Tertiary Laramide orogeny resulted in pervasive brittle deformation and erosion of the Cheyenne belt west of the Sierra Madre (E.M. Duebendorfer, pers. comm., 1987).

Local geology

In the vicinity of the New Rambler deposit, intermediate to mafic plutonic rocks have undergone variable degrees of metamorphism, deformation and

hydrothermal alteration. The predominant rock type in the area is amphibolitized metagabbro of the Mullen Creek mafic complex (MCMC) (Fig. 1). The MCMC is an irregularly shaped body of mafic rocks formed in an island-arc setting and accreted during the Proterozoic (Karlstrom & Houston 1984). The MCMC is truncated to the northwest by the Cheyenne belt. In highly deformed areas of the Cheyenne belt, olivine metagabbro grades into foliated amphibolite. Other rock types in the area of the New Rambler deposit include biotite–epidote–plagioclase gneiss, diabase dikes, and variably deformed granitic and quartz monzonitic stocks. The structure in the area is dominated by a series of intersecting shear-zones of the Cheyenne belt in which the degree of metamorphism and alteration of country rock is directly related to the intensity of deformation (Houston 1968, McCallum *et al.* 1976).

Geometry and structure of the New Rambler orebody are poorly known because the deposit has been inactive since the early 1900s, and most of the mining records were destroyed by a fire in 1918. Kemp (1904) reported that the majority of the ore was extracted from three large, irregular ore pods within altered and deformed metagabbro and metadiorite. The pods were discontinuous, showing no consistent trend between them, and were located at the intersections of mylonite zones and brittle fractures. The first pod was dome shaped, containing an upper zone of iron oxides and a lower zone of copper carbonates, sulfates and oxides, chrysocolla, native copper and only minor amounts of sulfides. The other two ore pods, located just east of the first, consisted of predominantly massive sulfides. Kemp (1904) hypothesized that the eastern two ore pods formed by "the decomposition of an eruptive dike in place", although McCallum *et al.* (1976) reinterpreted the structures to be tectonically emplaced blocks of the Mullen Creek mafic complex.

Paragenesis of the New Rambler Mine

Ore mineralogy

In a detailed study of ore minerals from mine dump samples, Loucks (1976) and McCallum *et al.* (1976) classified the primary ore into three assemblages. The following is a brief summary of the mineralogy and textures described by Loucks (1976) and McCallum *et al.* (1976).

Assemblage 1 consists principally of coprecipitated pyrite, magnetite and pyrrhotite, with traces of chalcopyrite and pentlandite. Assemblage 1 occurs in massive sulfide bodies and as disseminated sulfides in quartz–sericite altered wallrock (Loucks 1976). Pyrite in assemblage 1 contains bimineralic pyrrhotite–chalcopyrite inclusions interpreted by McCallum *et al.* (1976) as exsolution products from a once homogeneous phase (intermediate solid-solution) enclosed within pyrite. Based on annealing experiments for pyrite grains that exhibit similar textures and compositions, and published data in the Cu–Fe–S system, McCallum *et al.* (1976) estimated that the observed textures and associated *PGE* mineralization formed at approximately 334°C. Assemblage 1 contains no *PGM*. Assemblage 2 contains abundant chalcopyrite, pyrrhotite and pyrite, with accessory minerals that include sphalerite, mackinawite, pentlandite, thiospinel, electrum and four *PGM*. This assemblage also occurs in massive sulfide bodies and as small, irregular disseminations in the altered mafic rocks. The mineralogy of assemblage 3 is similar to that in assemblage 2, with a texturally distinct base- and precious-metal mineral assemblage. In addition to the major sulfide minerals of assemblage 2, assemblage 3 contains magnetite, native silver and seven *PGM*. A supergene ore assemblage also was identified by McCallum *et al.* (1976).

Platinum-group minerals at New Rambler occur as arsenides, tellurides and bismuthotellurides. The four *PGM* in assemblage 2 include rhodian sperrylite, merenskyite, kotulskite and michenerite. Merenskyite is the most common *PGM* in assemblage 2 and invariably contains small, discontinuous exsolution-lamellae of kotulskite oriented parallel to the {0001} cleavage (McCallum *et al.* 1976). All other *PGM* in assemblage 2 occur as anhedral grains enclosed within chalcopyrite or its supergene equivalents covellite or limonite. The *PGM* in assemblage 3 consist predominantly of a Pd bismuthotelluride [$Pd_5(Bi,Sb)_2Te_4$], plus minor amounts of michenerite, merenskyite, kotulskite, sperrylite, moncheite, and an unnamed mineral with the formula $Pd_5(Te,Bi,Sb)_2$. *PGM* in assemblage 3 occur as small grains within chalcopyrite and pyrrhotite and as small inclusions within other *PGM*.

Wallrock alteration and quartz segregations

McCallum *et al.* (1976) described two hypogene alteration assemblages and a "supergene" alteration assemblage within wall rocks at New Rambler. All samples investigated by McCallum *et al.* (1976) and in this study show propylitic alteration, with the development of chlorite + epidote + clinozoisite + albite + magnetite ± pyrite. The second alteration assemblage, characterized by the presence of quartz + sericite + pyrite, occurs adjacent to silicified zones that McCallum *et al.* (1976) interpreted as "fluid-bearing channels". Disseminated chalcopyrite also is present within the phyllic alteration assemblage. Both types of wallrock alteration intensify adjacent to zones of Cu and *PGE* mineralization (Loucks 1976). Late "supergene" processes, consisting of silicification and oxidation of the primary minerals and alteration assemblages, have been

reported by McCallum *et al.* (1976).

Samples used in this study for fluid-inclusion microthermometric analysis show varying degrees of alteration. The metagabbro has a relict subophitic texture, although several samples exhibit a weak to moderate fabric. Metagabbro has been amphibolitized during regional metamorphism and shearing, and consists predominantly of amphibole and plagioclase. The metamorphic assemblage has been overprinted by propylitic and phyllic alteration. A few relict clinopyroxene grains also are present in some of the less altered metagabbro.

Quartz segregations, present in many samples of altered metagabbro, occur as pods, veins and small inclusions within altered amphibole grains. Propylitic and phyllic alteration of amphibole and feldspars, especially chloritization of amphibole, typically increases adjacent to the quartz segregations, indicating that quartz deposition occurred during wallrock alteration and mineralization. In thin section, quartz exhibits abundant evidence of ductile deformation, with development of undulatory extinction, grain-size reduction, recrystallization and formation of core–mantle structures. Boundaries between quartz grains are highly irregular and usually marked by granulated rims. Microstructural and mineralogical textures indicate that hydrothermal alteration and mineralization were syntectonic.

Sulfides within quartz segregations include pyrite ± chalcopyrite ± galena ± pyrrhotite. Both pyrite and chalcopyrite occur as small grains disseminated in the quartz veins. Galena and pyrrhotite are present as rims around some of the larger sulfide grains. Pyrite + chalcopyrite + pyrrhotite are the dominant sulfide phases in ore assemblage 1 of McCallum *et al.* (1976), although galena had not been previously reported. Magnetite also occurs as small disseminated grains in quartz and commonly is oxidized to hematite + ilmenite. McCallum *et al.* (1976) also described accessory martitized magnetite as part of assemblage 3.

McCallum *et al.* (1976) proposed that the three mineral assemblages were deposited as a continuum over a small temperature interval ranging from 334°C for assemblage 1 to 300–334°C for assemblages 2 and 3. No *PGM* were found in the samples studied for this project, but the similarity of sulfide and oxide minerals to assemblages 1 and 3 of McCallum *et al.* (1976) is consistent with quartz deposition during Cu and *PGE* mineralization.

Fluid Inclusions in Quartz Segregations

Samples collected from the mine dump at the New Rambler deposit were sectioned for both fluid-inclusion microthermometry and detailed petrography. Petrography permitted identification of the alteration assemblages, the types and distribution of fluid inclusions, and the nature of microstructures in quartz. Sulfide and oxide phases were identified by reflected-light petrography. Temporal relationships among populations of fluid inclusions were determined using cross-cutting features such as planes of fluid inclusions intersecting or cross-cutting older clusters. Intersections of planes of fluid inclusions are commonly characterized by groups of decrepitated inclusions.

Microthermometric data were collected on a USGS-type gas-flow heating–freezing stage adapted by Fluid Inc. The stage was calibrated at –56.6, 0 and 374.1°C using synthetic fluid inclusions (Bodnar & Sterner 1985).

Petrography and microthermometry

Quartz deposition during hydrothermal alteration suggests that the fluids that produced wallrock alteration and quartz segregations are the same fluids that remobilized the *PGE*. McCallum *et al.* (1976) reported difficulty in separating "supergene silicification" from silicification associated with zones of phyllic alteration. However, microstructures observed in quartz segregations require quartz deposition prior to, or during, at least some of the deformation. Furthermore, the observed increase in degree of chloritization of amphibole and sericitization of feldspars adjacent to quartz segregations indicates a genetic link between silica deposition and hydrothermal alteration.

The small size of fluid inclusions in feldspar and amphibole prohibited microthermometric measurements; therefore, all fluid-inclusion data were collected from inclusions in quartz. Fluid inclusions in quartz segregations are found as isolated clusters and along well-healed as well as poorly healed fractures. In general, fluid inclusions are best preserved in planes within the cores of the core–mantle structures that are truncated along grain boundaries. The texture suggests that fluids were trapped in inclusions prior to the end of deformation. Fluid inclusions also are found in planes along and cross-cutting subgrain boundaries as well as within quartz inclusions in altered amphibole.

Three types of fluid inclusions were identified in the quartz segregations. Based on cross-cutting relationships and association with alteration assemblages, type-1 inclusions are the oldest, or first trapped, and those of type 3 are the youngest.

Type 1: nitrogen inclusions

Type-1 fluid inclusions are dark, single-phase inclusions at room temperature. They are found in planes and irregular clusters confined to single quartz grains. The N_2 inclusions have an irregular to nega-

tive crystal shape, range in size from <5 to 15 μm, and are relatively rare compared with the other types of inclusions. No phase changes were observed during microthermometric analysis; however, Raman microspectroscopy confirmed the presence of nitrogen. No other species were detected using Raman analysis.

Type 2: carbon dioxide inclusions

One- and two-phase CO_2 inclusions, at room temperature, occur singularly within individual grains, along well-healed fractures that are truncated by grain boundaries, and in irregular clusters. CO_2 inclusions range in size from <1 μm up to 15 μm, have irregular to round shapes and are relatively rare in comparison to the aqueous (type 3) inclusions discussed below. No aqueous phase was observed in type-2 inclusions, but owing to the small size of the inclusions, an undetected aqueous phase may have been present.

Figure 2A shows the temperature of final melting of the CO_2 inclusions. There is no compositional difference between the texturally distinct occurrences of these inclusions. Most type-2 inclusions exhibit melting temperatures that cluster at -56.6°C, the triple point of pure CO_2. However, where spatially associated with the type-1, N_2 inclusions, the CO_2 inclusions exhibit melting temperatures that are depressed from the CO_2 triple point by as much as 5°C. Depressed melting temperatures may result from mixing of fluids from opened N_2 inclusions during trapping of CO_2 inclusions. The few CO_2 inclusions that were analyzed using the Raman microprobe did not show discernible N_2 or CH_4 peaks.

Homogenization temperatures (Th) of the CO_2 inclusions are shown in Figure 2B. All of the CO_2 fluid inclusions homogenized to liquid, with distinct populations at 26–31°C, 14–18°C and an asymmetrical distribution with a major peak at 8–10°C. The distribution of homogenization temperatures may be the result of natural variations in density, contamination by N_2, or re-equilibration of inclusions after trapping.

Type 3: aqueous inclusions

Type-3 inclusions are, by far, the most abundant in the quartz segregations. Microthermometric analysis has outlined two types of aqueous inclusions; those of high salinity (type 3A) and those with low salinity (type 3B). The high-salinity inclusions have been further subdivided into inclusions that are saturated with respect to NaCl at room temperature and those that are not. The high-salinity aqueous inclusions (type 3A) are more abundant than the low-salinity variety (type 3B).

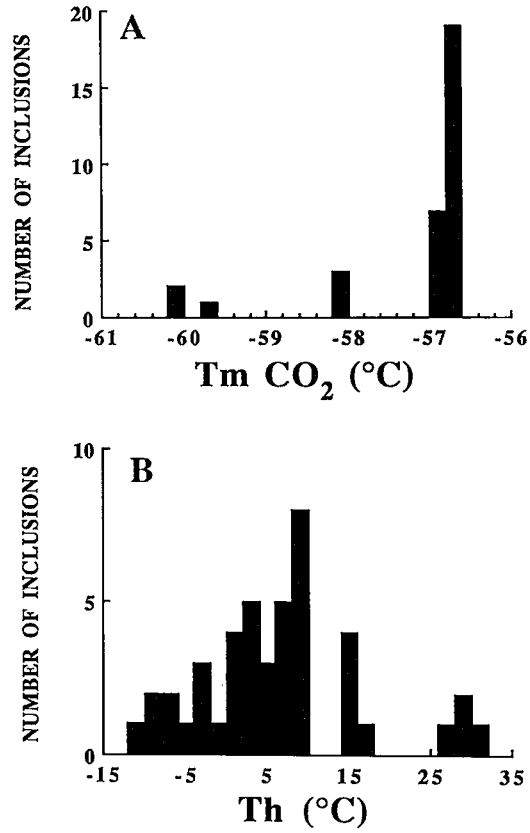

FIG. 2. (A) Histogram showing final melting temperatures of CO_2 fluid inclusions. The peak at -56.6°C indicates that fluid inclusions contain pure CO_2. The fluid inclusions that show depressed melting temperatures occur near N_2 inclusions and may contain trace amounts of N_2. (B) Histogram showing homogenization temperatures of CO_2 fluid inclusions. See text for discussion.

Type 3A: high-salinity (H_2O–NaCl–$CaCl_2$) inclusions

Both types of high-salinity inclusions occur along well-healed fractures, which are commonly truncated at grain boundaries, and in irregular clusters, which are adjacent to areas of increased alteration of the wallrock. Small (<5 μm) high-salinity inclusions also occur as individuals and small groups of inclusions in quartz contained within amphibole grains. The presence of halite as a daughter mineral in these inclusions characterizes the inclusions as type 3A. However, the small size precluded microthermometric analysis. The high-salinity inclusions form negative crystal to irregular shapes.

Temperatures of first melting for the two-phase and three-phase inclusions were observed between -44 and -50°C, indicating that the fluids can be

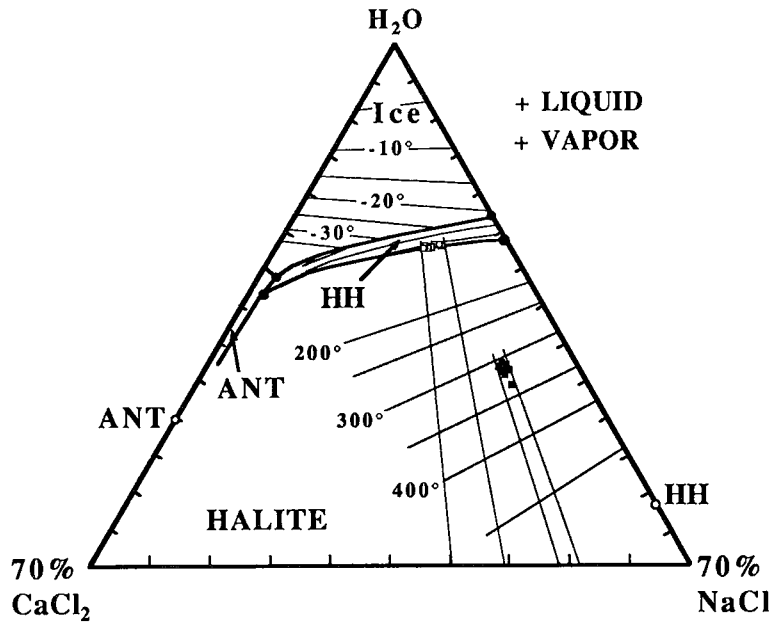

FIG. 3. Phase diagram for the H_2O–NaCl–$CaCl_2$. Open squares represent bulk compositions of two-phase type-3A inclusions, and filled squares represent bulk compositions of three-phase type-3A inclusions, which contain a halite daughter mineral. The light solid lines that cross the halite + liquid field outline the $CaCl_2/(CaCl_2+NaCl)$ weight ratio for each population of inclusions. Isotherms are plotted from data of Yanatieva (1946) for the hydrohalite (HH) + liquid field, Vanko *et al.* (1988) for the halite + liquid field, and Oakes *et al.* (1990) for the ice + liquid field. Cotectic boundaries between the Ice + HH, HH + Halite, Antarcticite (ANT) + Ice, ANT + HH and ANT + Halite fields are from Yanatieva (1946).

modeled in the H_2O–NaCl–$CaCl_2$ system (Crawford 1981, Vanko *et al.* 1988, Oakes *et al.* 1990). First melting of the two-phase inclusions is recognized by a change in the shape of the coarse crystalline ice, followed by substantial melting. As the quantity of ice decreases, hydrohalite becomes more recognizable and appears as small, dark-rimmed crystals with higher relief than ice. With continued heating, ice always melts prior to melting of hydrohalite; therefore, the bulk composition of the fluid inclusion must plot in the hydrohalite field because halite daughter minerals are absent (Fig. 3). Ice melting occurs between -41.0 and -25.0°C, and hydrohalite melts between -9.6 and -7.0°C. These observations and the range in temperature of final melting restrict the total salinity of the inclusions to 26–27 wt. %, with a $CaCl_2/(CaCl_2+NaCl)$ weight ratio of 0.3–0.4.

Three-phase (liquid–vapor–halite) inclusions exhibit characteristics and temperatures of first melting similar to the two-phase inclusions. Coarse ice crystals first round at the corners and then completely melt prior to hydrohalite melting. During the stage of ice melting, between -41.0 and -26.4°C, both hydrohalite and halite daughter minerals become larger. With continued heating, the hydrohalite melts between -9.6 and -7.5°C. Further heating reduces the size of the halite daughter phase, with final dissolution occurring between 317 and 340°C. This sequence of phase changes and the range of temperatures correspond to a total salinity of 42–45 wt.% and a $CaCl_2/(CaCl_2+NaCl)$ weight ratio of approximately 0.20 (Fig. 3).

Total homogenization temperatures for all high-salinity inclusions range from 335 to 365°C, with homogenization to the liquid. Vapor bubbles in the three-phase inclusions always homogenize after dissolution of halite daughter crystals.

The origin and relationship between the two groups of high-salinity inclusions are not clear. The two-phase inclusions may represent a separate population of inclusions with salinities intermediate between type-3B low-salinity inclusions (see below) and three-phase type-3A high-salinity inclusions. Conversely, because all type-3A inclusions fall along a tie line extending from NaCl to the melting temperature of hydrohalite, it can be argued that type-3A

inclusions may represent a single population. Differences in the phases present at room temperature, *i.e.*, the presence or absence of halite, may be a function of metastability (Touray & Sabouraud 1970).

Type 3B: low-salinity (H_2O–NaCl) inclusions

Low-salinity inclusions are younger than the high-salinity type, as planes of low-salinity inclusions cross-cut and offset zones containing halite-bearing inclusions. Populations of low-salinity inclusions are found along poorly healed fractures that cross-cut grain boundaries in the deformed quartz segregations but that do not penetrate the altered host-rock. No low-salinity inclusions were found in quartz within the altered amphibole grains. Low-salinity inclusions have highly irregular shapes.

Low-salinity inclusions exhibit normal heating and freezing behavior. Temperatures of first melting between -20 to -21°C were detected by the rounding of ice crystals within the inclusions. Temperatures of final ice melting range from -1.3 to -7.3°C (Fig. 4A), corresponding to 2–10 wt.% NaCl equivalent.

Final homogenization of the two-phase, low-salinity inclusions is to the liquid phase and exhibits a mode at approximately 155°C, with several subsidiary peaks (Fig. 4B). In general, homogenization temperature is consistent within a cluster or plane of fluid inclusions but varies among different clusters or planes. Variation in homogenization temperatures may be due to necking or re-equilibration of inclusions during uplift or deformation, or may represent real variations in trapping temperature and pressure.

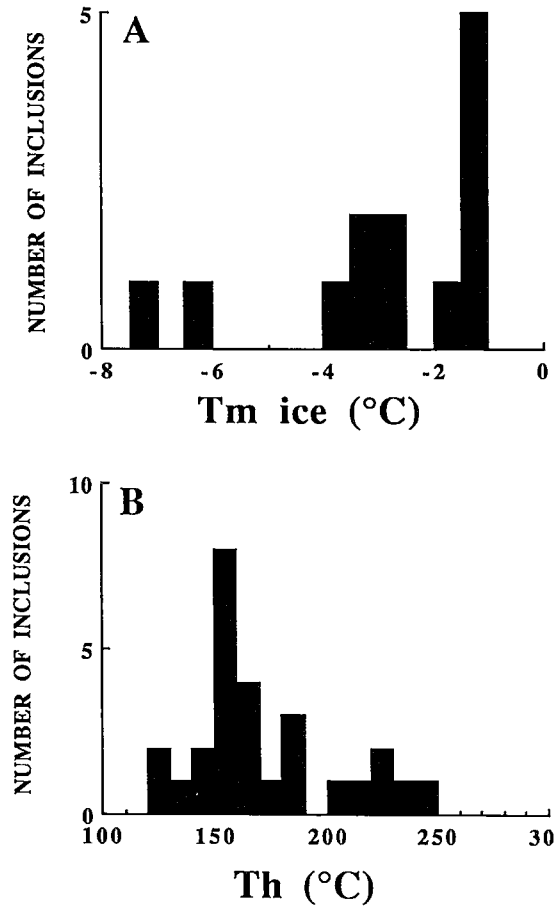

FIG. 4. Histograms of (A) the final ice melting temperatures and (B) the homogenization temperature of the low-salinity aqueous inclusions. See text for discussion.

DISCUSSION

Physicochemical constraints on mineralization

As stated previously, N_2 fluid inclusions formed early, followed by, or perhaps accompanied by, the CO_2 fluid inclusions. Textural evidence indicates that high-salinity inclusions postdate the N_2 and CO_2 inclusions but predate the low-salinity aqueous inclusions. High-salinity inclusions occur in quartz included in altered amphibole and in isolated quartz grains within the alteration sequences, and represent the fluids trapped during amphibolitization, propylitization and sericitization of the mafic wall-rocks. Petrographic relationships between the fluid inclusions and quartz microstructures indicate that the fluids were trapped prior to the end of deformation. The temperature of total homogenization for the high-salinity inclusions (335 to 365°C) provides a minimum estimate for the temperature of mineralization. These values are in excellent agreement with the minimum temperature of 334°C reported by McCallum *et al.* (1976) based on pyrrhotite–chalcopyrite exsolution found within pyrite for the early stage of sulfide mineralization. At this time, a pressure correction cannot be assigned to temperature estimates for mineralization at the New Rambler deposit. However, estimates of the maximum *P–T*, based on regional values from syntectonic metamorphic assemblages, must be between 300 and 475°C at pressures of 2500–3500 bars (Duebendorfer 1988). *P–V–T* properties for the H_2O–NaCl–$CaCl_2$ system are not available, but isochores for the type-3A inclusions modeled in the H_2O–NaCl system (Bodnar 1985) are consistent with *P–T* estimates from syntectonic mineral assemblages.

Fluid-inclusion data and information available from sulfide and oxide mineral assemblages found in the veins as well as reported in the ore (McCallum *et al.* 1976) can be used to constrain the physical and chemical conditions at the time of *PGM*

deposition in the New Rambler deposit. The high-salinity (type-3A) fluid inclusions contain between 5.2 and 11.9 molal chlorine. The $f(O_2)$, $f(S_2)$ and pH of the system are constrained by the ore-mineral assemblages (1–3) deposited with the *PGM* mineralization. Using data from Mountain & Wood (1988) for 300°C, and the association pyrite–pyrrhotite–magnetite found in ore assemblage 1 as well as within the quartz veins and pods, $f(O_2)$ seems to have been approximately 10^{-35}, and $f(S_2)$, approximately 10^{-11}. The occurrence of pyrite and pyrrhotite without magnetite, common in ore assemblage 2, requires similar $f(O_2)$ and $f(S_2)$ conditions, whereas the martitization of magnetite to hematite observed in ore assemblage 3 and within the quartz segregations indicates an increase in $f(O_2)$ to approximately 10^{-30}. The pH of the system constrained by the assemblage pyrite–pyrrhotite–magnetite is greater than 8 at 300°C, depending on the total concentration of sulfur in solution. The absence of magnetite in assemblage 2 requires a decrease in the pH relative to assemblage 1 (Barton 1984).

Theoretical models of *PGE* solubility are equivocal concerning the complexing agent for the *PGE*. Calculations by Mountain & Wood (1988) indicate that bisulfide complexes are most efficient at complexing Pt and Pd at 300°C, whereas Sassini & Shock (1990) present data indicating substantial solubility of the Pd by chloride complexes. Recent work on the Salton Sea geothermal system also favors mobility of *PGE* as chloride complexes (McKibben *et al.* 1989). In addition, the general physical and chemical conditions of Salton Sea geothermal brines within the reservoir (365°C, >25 wt.% total dissolved salts, log $f(O_2)$ of –30, and Cl-, Na- and Ca-rich brines; McKibben & Elders 1985) are very similar to those reported here for the New Rambler deposit, and supports *PGE* transport as chloride complexes at New Rambler. Given that 1) the intensity of alteration increases adjacent to zones of *PGE* mineralization (McCallum *et al.* 1976) and quartz segregations (this study), and 2) quartz within the highly altered rocks contains predominantly high-salinity inclusions, it is reasonable to postulate that fluids responsible for mineralization and alteration were chloride-rich brines. Furthermore, the presence of *PGE* as intermetallic compounds rather than sulfides supports transport by chloride rather than bisulfide complexes (C.G. Ballhaus, pers. comm., 1989).

Estimates of *PGE* solubility at New Rambler based on theoretical models are difficult. Large discrepancies exist between the physical and chemical conditions at the New Rambler deposit and conditions used in theoretical models. Mountain & Wood (1988) reported that Pt and Pd solubilities as chloride complexes at 300°C, at the pyrite–pyrrhotite–magnetite equilibrium, with 0.005 molal total sulfur in solutions and 1 molal total chloride, would be several orders of magnitude lower than their lowest reported solubility of 0.1 ppb. Pt and Pd solubilities in fluids responsible for mineralization at the New Rambler deposit are likely to be greater given the higher chloride molality indicated by the saline inclusions. Sassini & Shock (1990) reported substantially higher concentrations of Pd in solution than Mountain & Wood (1988), although at a lower pH than recorded by the New Rambler ore-mineral assemblages. McKibben *et al.* (1989) reported $\leq$0.3 ppb *PGE* in the Salton Sea geothermal system brines, which is three orders of magnitude greater than predicted by the theoretical models mentioned above. Thus, theoretical models and natural examples support *PGE* transport by chloride complexes at conditions similar to those for the New Rambler deposit.

McCallum *et al.* (1976) proposed a model for Cu and *PGE* mineralization at the New Rambler deposit involving remobilization and transport of *PGE* and Cu from the gabbroic country-rock and deposition within dilatant shear-zones during retrograde metamorphism and deformation. They proposed that decreases in pressure within the shear zone caused precipitation of Cu minerals and *PGM*. The results of this study indicate remobilization by chloride-rich brines. Deposition of *PGE* and Cu mineralization was probably facilitated by chemical reaction between mineralizing fluids and wallrock. The increased intensity of hydrothermal alteration assemblages adjacent to quartz segregations and mineralization supports this hypothesis. Also, C.G. Ballhaus (pers. comm., 1989) suggests that the interaction of more acidic, oxidized transporting fluids with a more reducing environment could produce a decrease in the *PGE* solubility and cause subsequent precipitation of the ore. Oxidation of magnetite to hematite observed with ore assemblage 3 and quartz veins provides evidence for the influx of an oxidizing fluid during *PGE* deposition.

Comparison with other hydrothermal PGE deposits

Fluid compositions of intermediate-temperature hydrothermal *PGE* deposits have not been well documented in previous studies; better constraints have been determined for high-temperature hydrothermal *PGE* deposits. Most notable of these are the studies of chlorine-rich hydrous silicates in the Bushveld and Stillwater complexes (Ballhaus & Stumpfl 1986, Stumpfl & Ballhaus 1986, Boudreau *et al.* 1986) and fluid-inclusion studies of the Bushveld Complex (Ballhaus 1985, Ballhaus & Stumpfl 1986, Schiffries 1985). Types of fluid-inclusions reported from the hydrothermal stage of the Bushveld mineralization include CH_4-bearing inclusions, CO_2-bearing inclusions, H_2O_2–NaCl inclusions and rare H_2O–CO_2–NaCl inclusions, with H_2O–NaCl inclusions being most common. Ball-

haus (1985) and Ballhaus & Stumpfl (1986) divided the H_2O–NaCl inclusions into three subgroups based on salinity. Schiffries (1985) reported temperatures of first melting of ice as low as –40°C, and Ballhaus (1985) and Ballhaus & Stumpfl (1986) reported various temperatures of first melting below the –21.2°C eutectic for H_2O–NaCl. The low temperatures of first melting indicate the presence of a divalent cation, most likely Ca or possibly Mg, in the fluid inclusions. The fluid-inclusion evidence agrees with the chlorine contents of hydrous silicates (Boudreau *et al.* 1986); thus substantial chlorine is available to form complexes that contribute to *PGE* transport in high-temperature hydrothermal *PGE* deposits.

Although inclusions in the hydrothermal portions of the Bushveld Complex were trapped under considerably different physical and chemical conditions than those at New Rambler, both data sets exhibit some gross similarities. Both deposits contain relatively pure condensed gaseous inclusions (CO_2, N_2 or CH_4), low-salinity aqueous inclusions and high-salinity aqueous brines. Aqueous brines are composed of NaCl and $CaCl_2(\pm MgCl_2)$. In both deposits, the high-salinity aqueous brines are the most abundant and are spatially and temporally associated with *PGE* mineralization and assemblages of hydrothermal minerals.

Conclusions

Four types of fluid inclusions have been identified within quartz segregations in hydrothermally altered mafic rocks at the New Rambler deposit. Based on the spatial and temporal relationships between high-salinity aqueous inclusions, alteration assemblages and *PGE* mineralization, high-salinity (type-3A) fluid inclusions contain the hydrothermal fluids trapped during ore formation. Homogenization temperatures fall within the range of 335 to 365°C and provide a minimum estimate of the temperature of mineralization. These temperatures are in accord with previous estimates of temperature based on sulfide mineralogy. Compositions of fluid inclusions from the New Rambler deposit are similar to those of fluid inclusions associated with the higher-temperature hydrothermal component of the Bushveld *PGE* mineralization. In addition, the fluid compositions and conditions reported in this study are similar to those of Salton Sea geothermal brines, which contain *PGE* transported as chloride complexes.

Evaluation of models of theoretical solubility using data from our fluid inclusions suggests a substantial solubility of *PGE* as chloride complexes in the New Rambler hydrothermal fluids, although the ranges of physical and chemical conditions used to construct the theoretical models do not overlap conditions at New Rambler. The lack of solubility data for conditions relevant to New Rambler, as well as other intermediate-temperature hydrothermal *PGE* deposits, highlights the need for additional experimental and theoretical studies over a wider range of P, T, $f(O_2)$, pH and salinity conditions, as well as the incorporation of data for important divalent cations such as Ca and Mg.

Acknowledgements

The authors thank A.J. Driscoll, Jr. for his initial help and input into this project. Raman analyses were provided by C.L. Knight in the Vibrational Spectroscopy Lab at VPI&SU. C.S. Oakes provided assistance with the interpretation of the high-salinity fluid inclusions and a review of early editions of the manuscript. J. Cline and D.L. Hall offered critical and constructive advice throughout the project. D.C. Sassini is thanked for supplying a preprint of his paper on Pd solubility. Constructive and helpful reviews by J. Dubessy, C.G. Ballhaus and R.F. Martin helped to clarify several points in the paper and are greatly appreciated.

References

Barton, P.P. (1984): Redox reactions in hydrothermal fluids. *Rev. Econ. Geol.* **1**, 99-113.

Ballhaus, C.G. (1985): Fluid inclusions in the Merensky Reef: significance for sulfide precipitation and platinum mineralization. *Fortschr. Mineral.* **63**, 15 (abstr.)

_____ & Stumpfl, E.F. (1986): Sulfide and platinum mineralization in the Merensky Reef: evidence from hydrous silicates and fluid inclusions. *Contrib. Mineral. Petrol.* **94**, 193-204.

Bodnar, R.J. (1985): *Pressure–Volume–Temperature–Composition (PVTX) Properties of the System NaCl–H_2O at Elevated Temperatures and Pressures.* Ph.D. dissertation, Pennsylvania State Univ., University Park, Pennsylvania.

_____ & Sterner, S.M. (1985): Synthetic fluid inclusions in natural quartz. II. Applications to *PVT* studies. *Geochim. Cosmochim. Acta* **49**, 1855-1859.

Boudreau, A.E., Mathez, E.A. & McCallum, I.S. (1986): Halogen geochemistry of the Stillwater and Bushveld complexes: evidence for transport of the platinum-group elements by Cl-rich fluids. *J. Petrol.* **27**, 967-986.

Cousins, C.A. (1973): Notes on the geochemistry of the platinum group elements. *Geol. Soc. S. Afr. Trans.* **76**, 77-81.

Crawford, M.L.(1981): Phase equilibria in aqueous fluid inclusions. *In* Fluid Inclusions: Applications

to Petrology (L.S. Hollister & M.L. Crawford, eds.). *Mineral. Assoc. Can., Short Course Handbook* **6**, 75-100.

DUEBENDORFER, E.M. (1988): Evidence for an inverted metamorphic gradient associated with a Precambrian suture, southern Wyoming. *J. Metamorph. Geol.* **6**, 41-63.

_____ & HOUSTON, R.S. (1987): Proterozoic accretionary tectonics at the southern margin of the Archean Wyoming craton. *Geol. Soc. Am. Bull.* **98**, 554-568.

HOUSTON, R.S. (1968): A regional study of rocks of Precambrian age in that part of the Medicine Bow Mountains lying in southeastern Wyoming, with a chapter on the relationships between Precambrian and Laramide structure. *Wyoming Geol. Surv. Mem.* **1**.

KARLSTROM, K.E. & HOUSTON, R.S. (1984): The Cheyenne Belt: analysis of a Proterozoic suture in southern Wyoming. *Precambrian Res.* **25**, 415-446.

KEMP, J.F. (1904): Platinum in the New Rambler mine, Wyoming. *U.S. Geol. Surv., Mineral Resources of the U.S.* **1902**, 244-250.

KUCHA, H. (1982): Platinum-group metals in the Zechstein copper deposits, Poland. *Econ. Geol.* **77**, 1578-1591.

LOUCKS, R.R. (1976): *Platinum-Gold-Copper Mineralization, Central Medicine Bow Mountains, Wyoming*. M.Sc. thesis, Colorado State Univ., Ft. Collins, Colorado.

MACDONALD, A.J. (1987): Ore deposit models #12. The platinum-group element deposits: classification and genesis. *Geosci. Canada* **14**, 155-166.

MCCALLUM, M.E., LOUCKS, R.R., CARLSON, R.R., COOLEY, E.F. & DOERGE, T.A. (1976): Platinum metals associated with hydrothermal copper ores of the New Rambler mine, Medicine Bow Mountains, Wyoming. *Econ. Geol.* **71**, 1429-1450.

MCKIBBEN, M.A. & ELDERS, W.A. (1985): Fe-Zn-Cu-Pb mineralization in the Salton Sea geothermal system, Imperial Valley, California. *Econ. Geol.* **80**, 539-559.

_____, WILLIAMS, A.E. & HALL, G.E.M. (1989): Au and PGE in Salton Sea geothermal brines. *Geol. Soc. Am. Abstr. Program* **21**, A294.

MOUNTAIN, B.W. & WOOD, S.A. (1988): Chemical controls on the solubility, transport, and deposition of platinum and palladium in hydrothermal solutions: a thermodynamic approach. *Econ. Geol.* **83**, 492-510.

NEEDHAM, R.S. & STUART-SMITH, P.G. (1987): Coronation Hill U-Au mine, South Alligator Valley, Northern Territory: an epigenetic sandstone-type deposit hosted by debris-flow conglomerate. *BMR J. Aust. Geol. Geophys.* **10**, 121-131.

OAKES, C.S., BODNAR, R.J. & SIMONSON, J.M. (1990): The system $NaCl-CaCl_2-H_2O$. I. The ice liquidus at 1 atm. total pressure. *Geochim. Cosmochim. Acta.* **54**, 603-610.

ORLOVA, G.P., RYABCHIKOV, I.D., DISTLER, V.V. & GLADYSHEV, G.D. (1987): Platinum migration in fluids during the formation of magmatic sulfides. *Int. Geol. Rev.* **29**, 360-362.

ROWELL, W.F. & EDGAR, A.D. (1986): Platinum-group element mineralization in a hydrothermal Cu-Ni sulfide occurrence, Rathbun Lake, northeastern Ontario. *Econ. Geol.* **81**, 1272-1277.

SASSINI, D.C. & SHOCK, E.L. (1990): Speciation and solubility of palladium in aqueous magmatic-hydrothermal solutions. *Geology* **17**, (in press).

SCHIFFRIES, C.M. (1982): The petrogenesis of a platiniferous dunite pipe in the Bushveld Complex: infiltration metasomatism by a chloride solution. *Econ. Geol.* **77**, 1439-1453.

_____ (1985): Reconnaissance study of fluid inclusions in the Bushveld Complex. *EOS Am. Geophys. Union Trans.* **66**, 418 (abstr.).

_____ & SKINNER, B.J. (1987): The Bushveld hydrothermal system: field and petrologic evidence. *Am. J. Sci.* **287**, 566-595.

STUMPFL, E.F. (1986): Distribution, transport and concentration of platinum group elements. *In* Metallogeny of Basic and Ultrabasic rocks (M.J. Gallagher, R.A. Ixer, C.R. Neary & H.M. Prichard, eds.). Inst. Min. Metall., London (379-394).

_____ & BALLHAUS, C.G. (1986): Stratiform platinum deposits: new data and concepts. *Fortschr. Mineral.* **64**, 205-214.

TOURAY, J.C. & SABOURAUD, C. (1970): Metastable inclusion brines in fluorite from Ouezzanne. *Econ. Geol.* **65**, 216-219.

VANKO, D.A., BODNAR, R.J. & STERNER, S.M. (1988): Synthetic fluid inclusions. VIII. Vapor-saturated halite solubility in part of the system $NaCl-CaCl_2-H_2O$, with application to fluid inclusions from oceanic hydrothermal systems. *Geochim. Cosmochim. Acta* **52**, 2451-2456.

YANATIEVA, O.K. (1946): Polythermal solubilities in the system $CaCl_2-MgCl_2-H_2O$ and $CaCl_2-NaCl-H_2O$. *Zh. Priklad. Khim.* **19**, 709-722 (in Russ.).

Received September 14, 1989, revised manuscript accepted April 6, 1990.